Indian Journal of Pure & Applied Physics
Vol. 55, February 2017, pp. 113-121

Synthesis, characterization and optical properties of CdSe/CdS and CdSe/ZnS core-shell nanoparticles

D K Gupta[a,b]*, M Verma[b], K B Sharma[b] & N S Saxena[b]

[a]Centre for Converging Technologies, University of Rajasthan, Jaipur 302 004, India

[b]Semiconductor and Polymer Science Laboratory, Department of Physics, University of Rajasthan, Jaipur 302 004, India

Received 24 August 2016; revised 16 November 2016; accepted 5 December 2016

Controlled organic synthesis method used for the preparation of cadmium selenide (CdSe) quantum dots, which are covered with cadmium sulfide (CdS) and zinc sulfide (ZnS) using TOP mediated has been presented in this paper. The size, shape, internal structure, chemical composition and functional groups of the core-shell nanoparticles were analyzed using X-ray diffraction, transmission electron microscopy, high resolution transmission electron microscopy, energy dispersive spectra and FTIR. These studies show that the particle size is in 2-10 nm range with hexagonal phase. The optical properties were analyzed through UV-visible spectroscopy, photoluminescence spectroscopy and micro-Raman spectroscopy. Photoluminescence blue shift and broadening of Raman spectrum further confirm the narrow size of particles.

Keywords: Core-shell nanoparticles, Organic synthesis, Transmission electron microscopy, Crystal structure

1 Introduction

The quantum dot is zero dimensional semiconducting nanocrystal whose radius is smaller than the bulk Bohr exciton radius. The electronic and optical properties of these nanomaterials show a significant change from their corresponding bulk properties, which are called quantum size effects. These QDs make a class of materials intermediate between molecular and bulk forms of matter. Quantum confinement of both the electron and hole in all three dimensions leads to an increase in the effective band gap of the material with decreasing crystallite size. The optoelectronic properties of semiconductor nanocrystals or quantum dots are dimension dependent in the nanometer range such as size dependent band gap, which leads to control and tune material's properties. Consequently, both the optical absorption and emission of quantum dots shift to the blue (higher energies) as the size of the dots gets smaller due to more pronounced quantum properties. Due to broad absorption spectra, solar devices using quantum dots have more efficiency than others. Quantum dots have good transport and optical properties due to very sharp density of states, hence can be used for LED and LASER devices. Quantum dots can be used for different applications due to their size and shape dependent properties such as display devices, photovoltaic, lasers and biomedical imaging[1-9]. CdSe quantum dots (QDs) have attracted interest in the fields of optoelectronics and biomedical imaging due to their wide absorption cross sections and narrow emission bands[10-11].

Semiconductor nanocrystals (SNCs) have drawn considerable attention due to the formation of core-shell nanoparticles[12]. The QDs require an emission that is stable against photo and chemical degradations for the use as light emitters. These characteristics can be achieved by coating the QD surface with inorganic materials which have a broader band gap that encompasses the band gap of the core QD[13-14].

Overcoating of nanocrystals with higher band gap inorganic materials can be used to improve the photoluminescence quantum yields by passivating surface non-radiative recombination sites. Particles passivated with inorganic shell structures are more robust than organically passivated dots and have greater efficiency to process the conditions required for integration into solid state structures[15-23]. Some examples of core-shell nanoparticle structures reported include CdS on CdSe and CdSe on CdS[15], ZnS grown on CdS[16], ZnS on CdSe and the inverse structure[17], CdS/HgS/CdS quantum dot quantum wells[18], ZnSe over coated CdSe[19], and SiO2 on Si[20-22]. This paper describes the synthesis and characterization of high quality core-shell (CdSe/CdS; CdSe/ZnS)

*Corresponding author
(E-mail: deepak.nanoconverge@gmail.com)

nanoparticles. CdS and ZnS over coated dots are characterized spectroscopically and structurally using a variety of techniques like UV-Vis, PL, XRD, TEM, EDX, FTIR and Raman. In addition to having higher efficiencies, CdS and ZnS over coated particles are more robust than organically passivated dots and potentially more useful for optoelectronic device structures. Electroluminescent devices (LED's) incorporating quantum dots (CdSe/ CdS or CdSe/ZnS) into heterostructure organic/semiconductor nanocrystallite light-emitting devices may show greater stability[23-24].

2 Experimental Method

2.1 Materials

Materials used were cadmium acetate dihydrate purified ($(CH3COO)_2Cd.2H_2O$, ≥98%, Merck), highly pure selenium powder (Se, 99.99% HPLC), trioctyl-n-phosphene oxide (TOPO, 99%, Aldrich), trioctyl phosphene (TOP, 97%, Aldrich), hexadecyl amine (HDA, 98%, Aldrich), tetradecyl phosphonic acid (TDPA, 97%, Aldrich), octadecene (ODE, 90%, TCI), oleic acid (Qualigens), oleylamine (Aldrich), toluene (≥99%, Merck), methanol (≥99%, Merck) etc.

2.2 Synthesis of CdSe nanocrystals

CdSe quantum dots were synthesized by the procedure developed by Ivo *et al.*[25] with some modification. In a typical recipe, 8 g of TOPO were taken in a 50 mL three neck flask. Then, 2.5 g HDA and 0.05 g TDPA were added, and dried at 100 °C for 15 min. The TOPSe stock solution was synthesized by mixing selenium 2 g in 5 mL of TOP and the mixture was heated to 270 °C. The cadmium stock solution (2.5g of $Cd(Ac)_2$ in 10 mL of TOP) was injected during stirring, resulting in nucleation of CdSe nanocrystals. Finally the red colored solution was obtained for CdSe QDs and washed several times with methanol, followed by centrifugation at 3000 rpm for 20 min. The purification was repeated three times. The above sediment was heated in vacuum at 70 °C for more than 48 h.

2.3 Synthesis of the CdSe/CdS core shell nanoparticles

Core-shell CdSe/CdS quantum dots were synthesized by the procedure developed by Cirillo *et al.*[26] with some modification**.** CdO (2.5 mmol) and oleic acid (5mmol) were mixed with 4 g of TOPO in a three neck flask. The reaction mixture was heated to 140 °C while flushing with nitrogen for two hour. The temperature was then increased to 330 °C. After the temperature had recovered, 4ml of a solution containing 100 mmol of CdSe core QDs and sulfur in TOP was injected. The sulfur was always kept in 4-fold excess as compared to cadmium. After 3 min, 10 mL of toluene was injected. The nanocrystals were purified by the addition of methanol, centrifugation at 4000 rpm for 20 min. The purification was repeated three times. The above sediment was heated in vacuum at 100 °C for more than 48 h.

2.4 Synthesis of CdSe/ZnS Core-shell nanoparticles

Core-shell CdSe/ZnS quantum dots were synthesized by the procedure developed by Zhu *et al.*[27] with some modification**.** A three-neck flask containing a mixture with 4 g of TOPO, 3 g of HDA, and 10 mL of ODE was heated to 100 °C under vacuum for 1 h and then cooled to 60 °C, and 0.08 mmol of CdSe QDs dispersed in toluene was transferred into the reaction vessel via a syringe. The toluene was removed under vacuum at 60 °C until bubbling in the mixture solution had ceased. The zinc precursor solution was prepared by dissolving zinc oxide (100 mg) in oleic acid (3 g) and ODE (10 mL) under a N_2 atmosphere at 320 °C and then kept in an oven at about 80 °C. The sulfur precursor solution was prepared by dissolving 40 mg of sulfur in 10 mL of ODE under N_2 flux at 180 °C and then cooled to room temperature. A zinc/sulfur mix solution was prepared by mixing 5 mL of zinc oxide solution with 5 mL of sulfur solution in a round bottom flask and keeping it warm (100 °C) in a heating mantle. The nanocrystals were purified by the addition of methanol, centrifugation at 4000 rpm for 20 min. The purification was repeated three times. The above sediment was heated in vacuum at 100 °C for more than 48 h.

2.5 Characterization techniques

The above synthesized core-shell nanoparticles were characterized for their crystal structure and phase using Panalytical Xpert Pro X-ray diffractometer (XRD) operating at 40 kV and 40 mA with λ = Cu-Kα (1.5418 Å) radiation in an angle range of 10° to 70°. Chemical bonding was investigated by using Fourier Transform Infrared spectroscopy (IR Affinity, Shimadzu). UV-visible (UV-Vis) spectra were recorded at room temperature using UV-Vis-IR spectrophotometer (Agilent Cary 5000 series) in the spectral range of 200 nm to 500 nm. Photoluminescence (PL) spectra were recorded using luminescence spectrometer (LS55-Perkin-Elmer) with a Xenon discharge lamp as

an excitation source and a grated photomultiplier tube as detector. Transmission electron microscopy (TEM) and high resolution electron microscopy (HRTEM) investigations were carried out using Tecnai 20 G^2 S-Twin TEM with *e*-beam voltage of 200 kV. The Raman spectra were taken using confocal micro-Raman model STR 500 (Airix Corporation) with solid state laser as a source having 532 nm wavelength and CCD detector.

3 Results and Discussion

3.1 Structural and morphological characterization

Figure 1 shows the XRD pattern of CdSe and core-shell (CdSe/CdS and CdSe/ZnS) nanoparticles. The XRD result of CdSe QDs measured in 10° to 70° angle range shows peaks at angles (2θ) 23.882°, 25.391°, 27.097°, 41.999°, 45.810°, 49.718°, 63.884° and 67.880° which correspond to planes (100), (002), (101), (110), (103), (112), (203), (211), respectively, and whose phase is found to be of hexagonal structure (a = 4.2990 Å = b, c = 7.0100 Å) according to JCPDS card no. 01-077-2307. Also broadening of the XRD pattern (peaks) is observed due to small dimensions of CdSe quantum dots.

In CdSe/CdS nanocrystals the positions of reflections from the CdS shell are shifted towards higher 2θ angles, which correspond to the expansion of CdS lattice and at high CdS coverage the appearance of a new peak at 36° and whose phase is found to be of hexagonal structure (a = 4.1360 Å = b, c = 6.7130 Å) according to JCPDS card no. 01-077-2306. Similarly, for the CdSe/ZnS nanoparticles the positions of reflections from the ZnS shell are shifted toward higher 2θ angles which corresponds to the expansion of ZnS lattice and at high ZnS coverage the appearance of a new peak at 56° and whose phase is found to be of Wurtzite structure (a = 3.8000 Å = b, c = 6.2300 Å) according to JCPDS card no. 00-003-1093. The broadening and small shift to higher 2θ is characteristic of the formation of core-shell (CdSe /CdS and CdSe/ZnS) nanocrystals and provides evidence that the synthesized (CdSe/CdS and CdSe/ZnS) nanoparticles described herein are core-shell nanoparticles.

From the XRD pattern, particle size of the CdSe and core-shell (CdSe/CdS and CdSe/ZnS) nanocrystals were determined using Eq. (1), Debye Scherrer relation:

$$D = \frac{0.9\lambda}{\beta \cos\theta} \quad \ldots (1)$$

where D, λ, β and θ are the particle size of QDs, wavelength of Cu-Kα radiation (1.5418 Å), full width

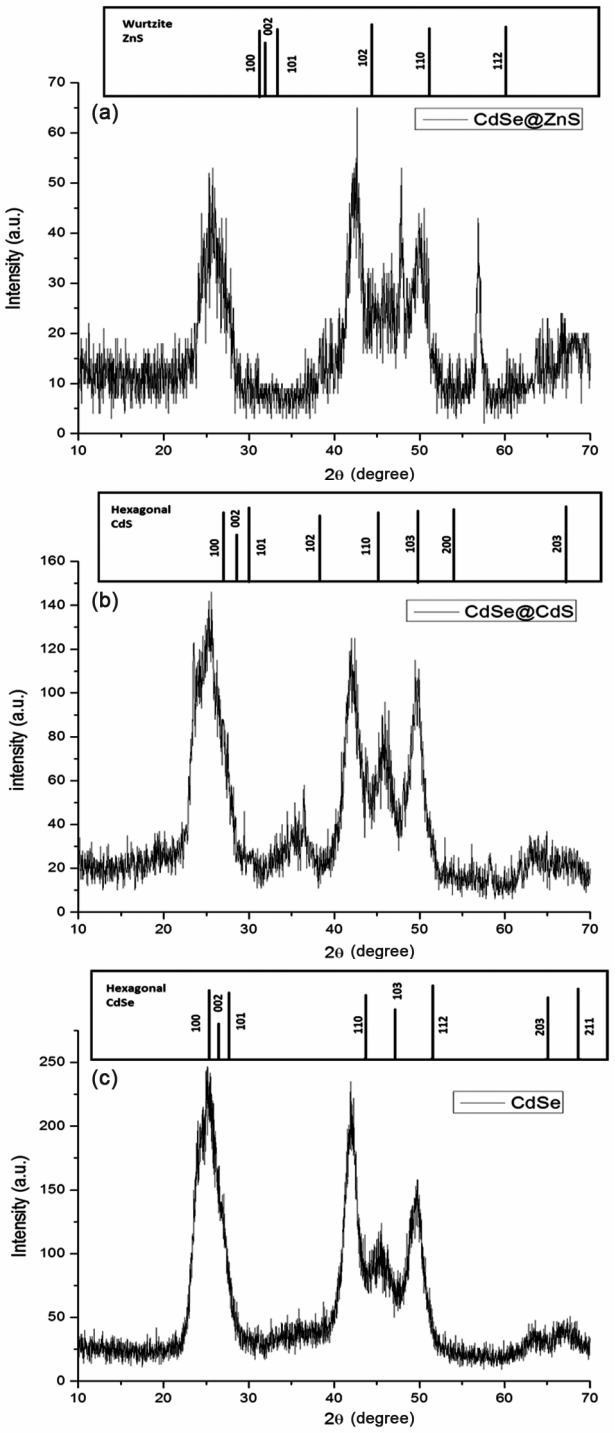

Fig. 1 – XRD diffraction pattern of CdSe, CdSe/CdS and CdSe/ZnS core-shell nanoparticles

at half maximum (FWHM) and angle corresponding to the peak, respectively. The average particle size as determined from XRD pattern was found to be 4.8 nm, 9.7 nm and 12.4 nm for CdSe, CdSe/CdS and CdSe/ZnS nanoparticles.

TEM, HRTEM images and SAED pattern for core CdSe nanocrystals and the CdSe/CdS and CdSe/ZnS core-shell nanoparticles are shown in Figs 2(a), (b) and (c). The CdSe/CdS nanoparticles have an average particle size diameter of 85 Å (an increase of 40 Å in relation to CdSe (45 Å)). The CdSe/ZnS (100Å) core-shell nanoparticles show an increase of 55 Å in relation to the parent material. This increase in particle size diameter is due to the growth of the shell.

Energy Dispersive X-ray (EDX) spectra of CdSe core nanoparticles and the same CdSe nanoparticles with CdS and ZnS shell grown on them are shown in the Figs 3(a), (b) and (c), respectively. Figure 3(b) and (c) shows the unambiguous evidence for the presence of Cd/Se/S and Cd/Se/Zn/S components.

FT-IR spectroscopy in Figs. 4(a), (b) and (c) was used to characterize the functional group present on the surface of the core CdSe nanoparticles and core-shell nanoparticles (CdSe/CdS and CdSe/ZnS). FTIR spectrum shows presence of the methyl group by the peaks at 2922 cm^{-1} which might be due to CdSe QDs in methanol solution. Others show 1035 cm^{-1} at C-N, 1526 cm^{-1} at N-H, 2335 cm^{-1} at P-H, 1720 cm^{-1} at C=O, 3305 cm^{-1} at O-H, 1178 cm^{-1} at P=O functional group, for the core CdSe nanoparticles and CdSe/CdS and CdSe/ZnS core-shell nanoparticles. Phosphene alkyl ligands provide repulsive interactions between the QDs in methanol, thus preventing aggregation.

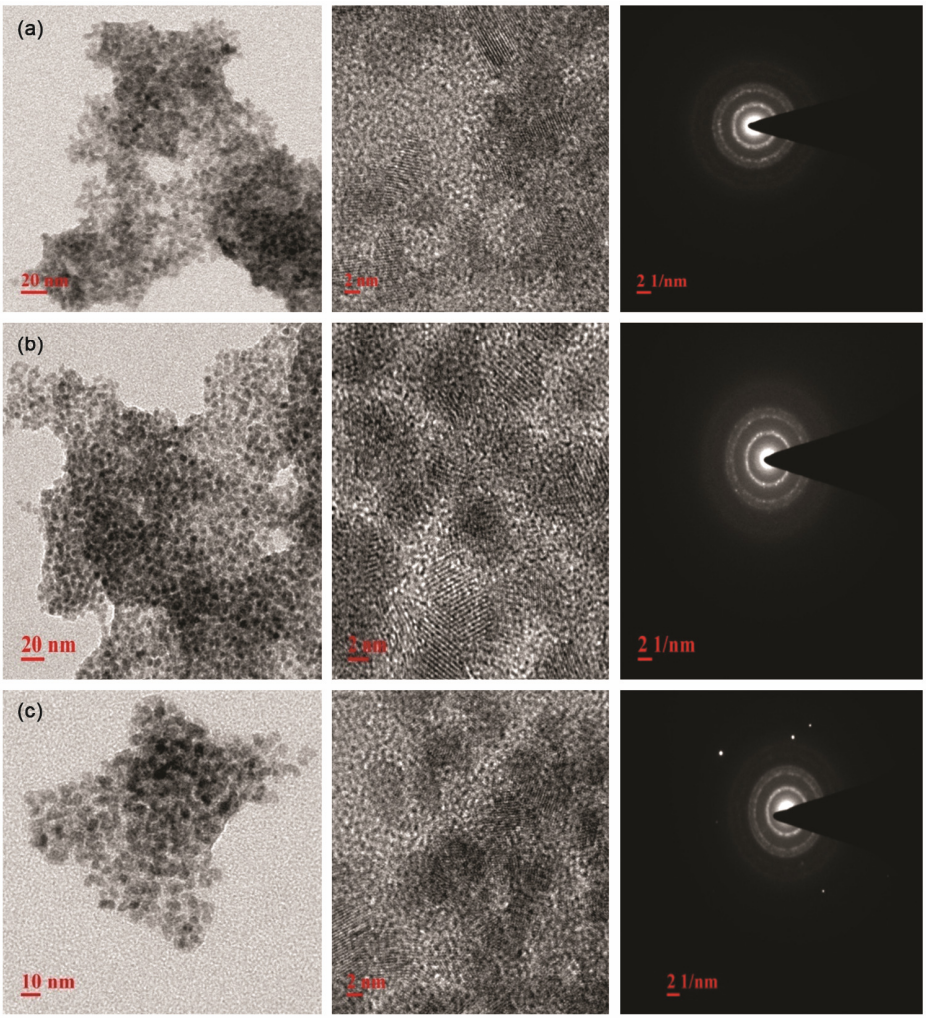

Fig. 2 – (a) TEM and SAED micrographs of CdSe QDs, (b) TEM and SAED micrographs of CdSe/CdS core-shell nanoparticles and (c) TEM and SAED micrographs of CdSe/ZnS core-shell nanoparticles

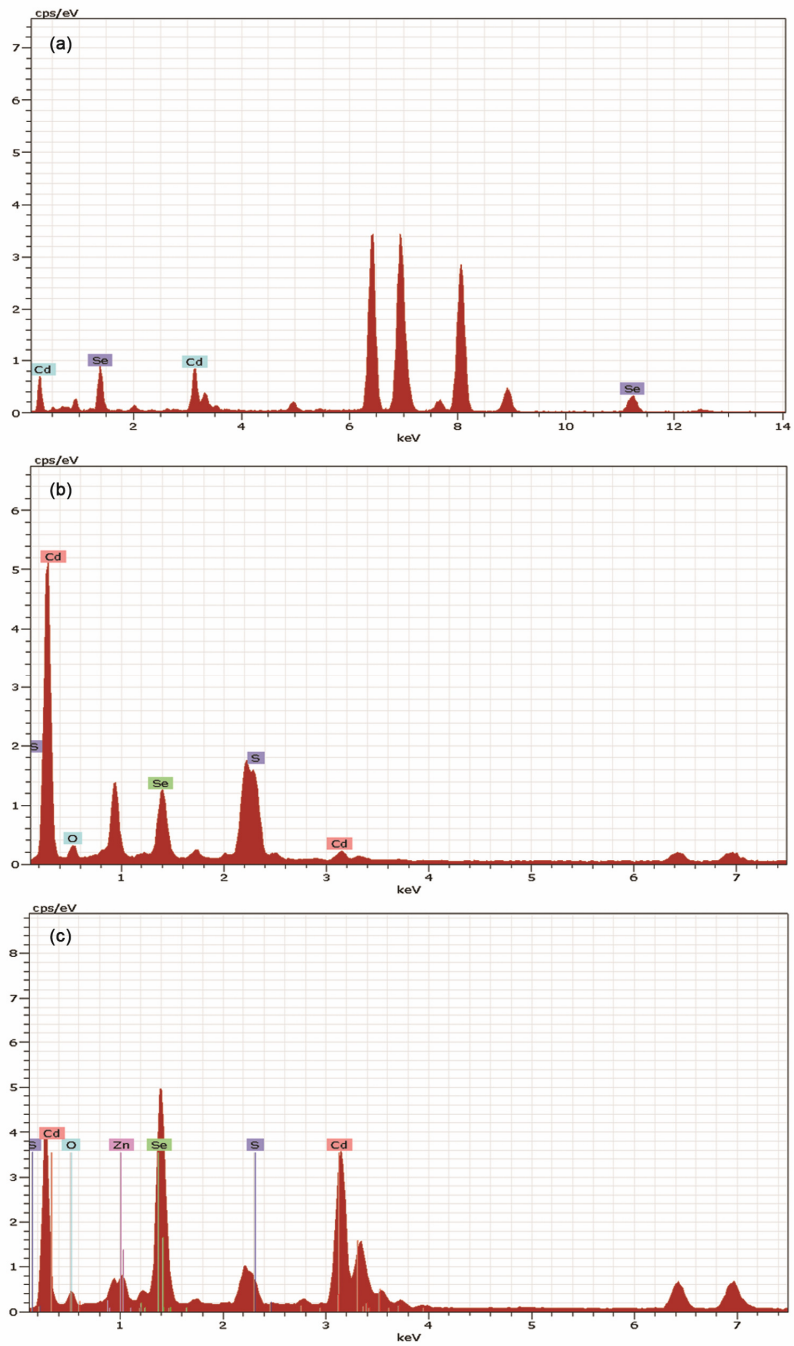

Fig. 3 – (a) EDX micrographs of CdSe QDs, (b) EDX micrographs of CdSe/CdS core-shell nanoparticles and (c) EDX micrographs of CdSe/ZnS core-shell nanoparticles

3.2 Optical studies

The growth of a shell around a core nanoparticle modifies the optical properties of the nanoparticle. The difference in the optical properties of the core-shell particles in comparison with those of the bare nanoparticles is evidence of shell growth. In this work, we compare the optical properties of the core-shell nanoparticles in relation to those of organically capped CdSe nanoparticles. The absorption spectra for CdSe, CdSe/CdS and CdSe/ZnS nanoparticles are shown in Fig. 5. The band edge is at 280 nm and 368 nm, a red shift of 20 nm and 108 nm compared to that of CdSe (260 nm) for CdSe/CdS and CdSe/ZnS nanoparticle, respectively. This red shift is indicative of the formation of the core-shell structure. The red shifts in the absorption spectra of the core-shell

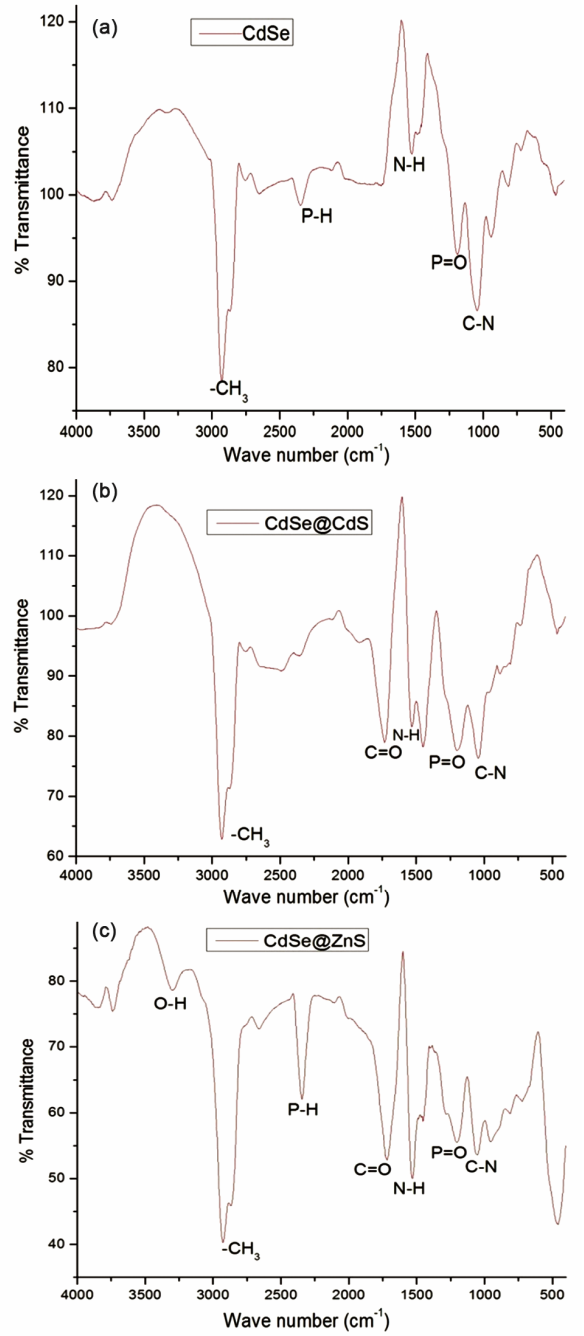

Fig. 4 – (a) FTIR spectra of CdSe quantum dots, (b) FTIR spectra of CdSe/CdS core-shell nanoparticles and (c) FTIR spectra of CdSe/ZnS core-shell nanoparticles

nanoparticles in relation to the parent material are attributed to relaxation of quantum confinement resulting from the growth of the shell.

These peaks are arising from the absorption of near band edge excitons. The absorption data were fitted to Tauc relation for near edge optical absorption of semiconductors:

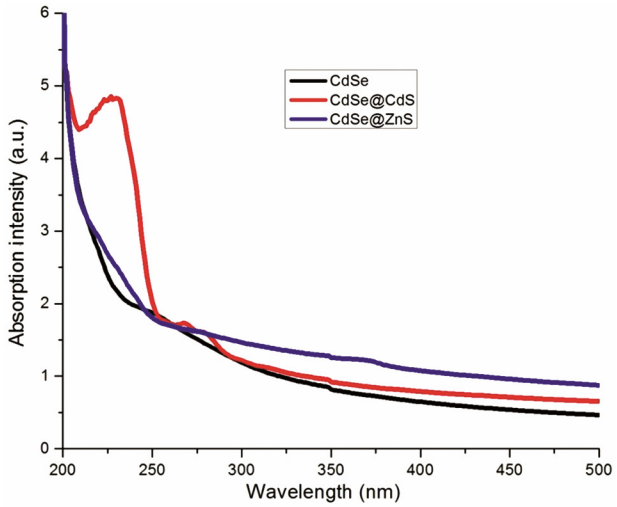

Fig. 5 – UV-Vis absorption spectra of CdSe, CdSe/CdS and CdSe/ZnS core-shell nanoparticles

$$a = \frac{(hv - E_g)^{\frac{n}{2}}}{hv} \quad \ldots (2)$$

In the above Eq. (2), E_g is optical band gap and n is a constant equal to 1 for direct band gap semiconductors. In Fig. 6(a), (b) and (c) plots for $(\alpha hv)^2$ versus hv for CdSe, CdSe/CdS and CdSe/ZnS nanoparticles have been shown and from these plots the band gap of CdSe was found to be 3.9 eV which shows blue shift (2.16 eV) compared to their bulk band gap of 1.74 eV. This blue shift can be explained on the basis of quantum size effect, i.e., the confinement of electron-hole in small region. Similarly band gap of CdSe/CdS and CdSe/ZnS nanoparticle were found to be 3.8 eV and 3.75 eV, respectively.

The photoluminescence spectra for CdSe, CdSe/CdS and CdSe/ZnS nanoparticles are shown in Fig. 7. The emission maximum of CdSe/CdS is at 568 nm, with that of CdSe/ZnS at 735 nm and that of CdSe at 564 nm. The emission maxima of the core-shell materials show red shifts in relation to the emission maximum of CdSe, consistent with the red shifts visible in the absorption spectra.

3.3 Micro-Raman studies

Raman spectra for the CdSe, CdSe/CdS and CdSe/ZnS samples are shown in Fig. 8(a), (b) and (c). It can be seen from Fig. 8 that the phonons are confined due to decrease in mean free path and Raman spectra are broaden which is a common characteristic of the II–VI nanomaterials with small dimensions. Lattice distortions and

structure defects of nanomaterials are also reasons to large broadening of Raman spectrum[28-30]. In Fig. 8(a) for CdSe QDs passivated by organic molecules reveal a Raman peak related to scattering by the longitudinal optical (LO) phonon at about 205 cm^{-1} which is red-shifted from its bulk value of 213 cm^{-1} due to phonon

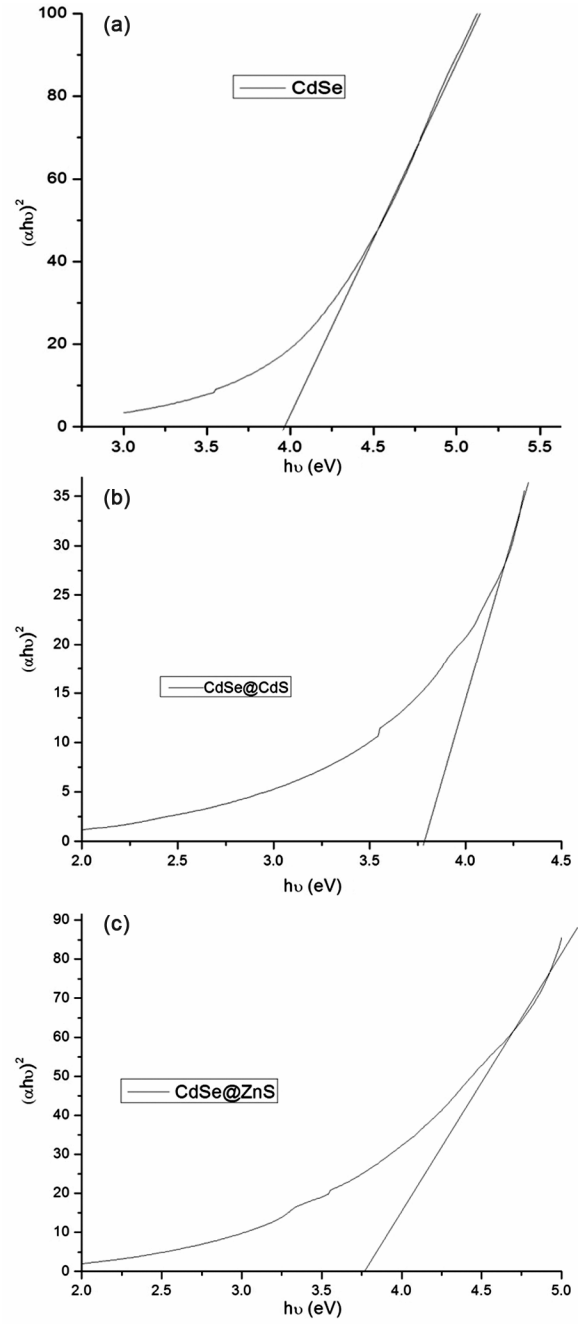

Fig. 6 – (a) Plot of $(\alpha h\nu)^2$ versus *hv* for CdSe QDs, (b) plot of $(\alpha h\nu)^2$ versus *hv* for CdSe/CdS core-shell nanoparticles and (c) plot of $(\alpha h\nu)^2$ versus *hv* for CdSe/ZnS core-shell nanoparticles

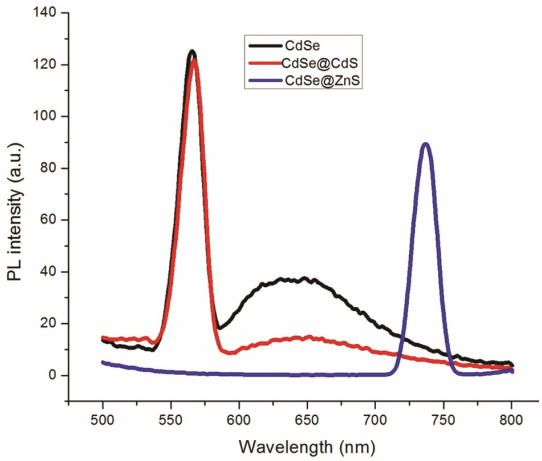

Fig. 7 – Photoluminescence spectra of CdSe, CdSe/CdS and CdSe/ZnS core-shell nanoparticles

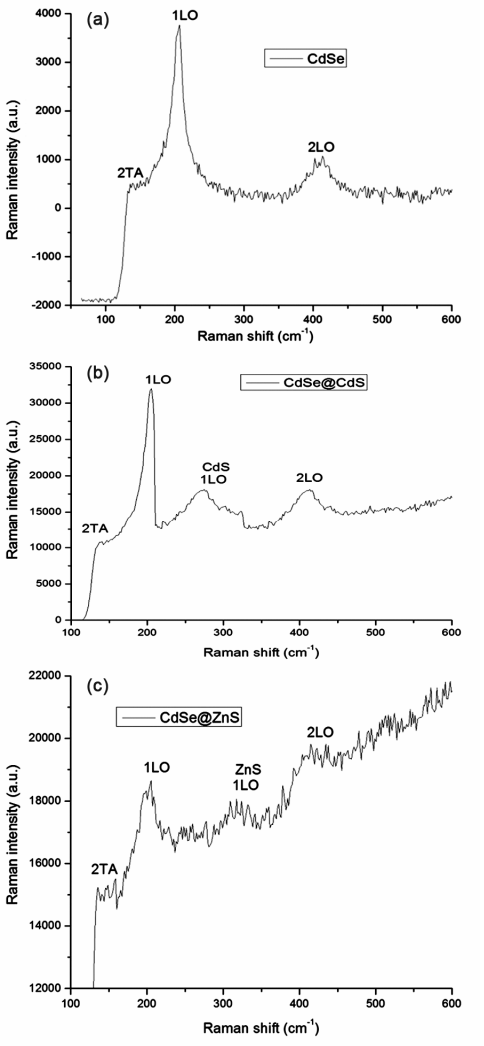

Fig. 8 – (a) Raman spectra of CdSe QDs, (b) Raman spectra of CdSe/CdS core-shell nanoparticles and (c) Raman spectra of CdSe/ZnS core-shell nanoparticles

confinement, as well as a weaker mode arising from the second order transverse acoustic (2TA), second order longitudinal optical (2LO) appeared at 134.49 cm^{-1} and 410.12 cm^{-1}, respectively.

The Raman lines of LO and 2LO phonons of the CdSe core and the line of LO phonons of the CdS and ZnS shell at about 270 cm^{-1} and 310 cm^{-1}, respectively, are clearly seen in the Fig 8(b) and (c), respectively. The Raman peak at 270 cm^{-1} was assigned to Cd–S vibrations in the shell. The Raman peak appeared at 270 cm^{-1} due to the Cd-S vibration, which downward shifted on 30 cm^{-1} from the bulk value of the CdS LO phonon, 305 cm^{-1}, due to the formation of an alloyed layer at the interface between CdSe core and CdS shell[31-33].

4 Conclusions

The core-shell structure of CdSe/CdS and CdSe/ZnS nanoparticles was synthesized successfully. These samples are analyzed optically and structurally using numerous techniques. The XRD pattern of bare CdSe QDs and core-shell nanoparticles confirmed the hexagonal phase. The elemental compositions of the bare and core-shell NPs are determined by EDX. The HRTEM micrographs of the core-shell nanoparticles give insight to the understanding of the formation of core-shell structure. The band gaps of CdSe, CdSe/CdS and CdSe/ZnS are found to be 3.9, 3.8 and 3.75 eV, respectively, from absorption spectra. The blue shifts in the PL emission spectra of the synthesized nanoparticles show size quantization effect. The synthesized core-shell nanoparticles show narrow and high PL emission due to passivation of surface nonradiative recombination sites. The Broad peaks of the Raman spectrum can be attributed to nanosize effects of the synthesized core-shell nanoparticles. These core-shell nanoparticles are therefore very promising for many applications where optical properties need to remain stable, such as lasing or biolabeling.

Acknowledgment

One of the authors Professor N S Saxena gratefully acknowledges UGC, New Delhi for providing financial support in the form of Emeritus fellowship. The authors also thank DST-FIST II for UV-Vis spectrophotometer.

References

1 Soloviev V N, Eichhoefer A, Fenske D & Banin U, *J Am Chem Soc,* 122 (2000) 2673.
2 Guzelian A A, J E B Katari, Kadavanich A V, Banin U, Hamad K, Juban E & Alivisatos A P, *J Phys Chem,* 100 (1996) 7212.
3 Banin, U, Cao Y W, Katz D & Millo O, *Nature,* 400 (1999) 542.
4 Yu H, Li J, Loomis R A, Gibbons P C, Wang L W & Buhro W E, *J Am Chem Soc,*125 (2003) 16168.
5 Peng X, Manna L, Yang W, Wickham J, Scher E, Kadavanish A & Alivisatos A P, *Nature*, 404 (2000) 59.
6 Li L L, Hu J, Yang W & Alivisatos A P, *Nano Lett*, 1 (2001) 349.
7 Verma M, Patidar D, Sharma K B & Saxena N S, *J Nanoelectron Optoelectron,* 10 (2015) 320.
8 Verma, M, Gupta D K, Patidar D, Sharma K B & Saxena N S, *Adv Sci Lett*, 21 (2015) 2657.
9 Gupta D K, Verma M, Patidar D, Sharma K B & Saxena N S, *Nanosci Nanotechnol Asia*, 6 (2016) 1.
10 Suganth A R B & Anjalin F M, *Der Pharma Chem*, 7 (2015) 67.
11 Medintz I L, Uyeda H T, Goldman E R & Mattoussi H, *Nat Mater,* 4 (2005) 435.
12 Peng A & Peng X, *J Am Chem Soc,* 123 (2001) 183.
13 Capek R K, Lambert K, Dorfs D, Smet P F, Poelman D, Eychmuller A & Hens Z, *Approach Chem Mater,* 21 (2009) 1743.
14 Tuinenga C, Jasinski J, Iwamoto T & Chika V, *ACS Nano*, 2 (2008) 1411.
15 Tian Y, Newton T, Kotov N A, Guldi D M & Fendler J, *J Chem Phys,* 100 (1996) 8927.
16 Youn, H C, Baral S & Fendler J H, *J Phys Chem,* 92 (1988) 6320.
17 Kortan, A R, Hull R, Opila R L, Bawendi M G, Steigerwald M L, Carroll P J & Brus L E, *J Am Chem Soc,*112 (1990) 1327.
18 Mews A, Eychmuller A, Giersig M, Schooss D & Weller H, *J Phys Chem,* 98 (1994) 934.
19 Danek M, Jensen K F, Murray C B & Bawendi M G, *Chem Mater,* 8 (1996) 173.
20 Littau K A, Szajowski P J, Muller A J, Kortan A R & Brus L E, *J Phys Chem,* 97 (1993) 1224.
21 Wilson W L, Szajowski P J & Brus L E, *Science,* 262 (1993) 1242.
22 Hines M A & Guyot-Sionnest P, *J Phys Chem,* 100 (1996) 468.
23 B O Dabbousi, J Rodriguez-Viejo, F V Mikulec, J R Heine, H Mattoussi, R Ober, K F Jensen & M G Bawendi, *J Phys Chem B,* 101 (1997) 9463.
24 Rodriguez-Viejo J, Jensen K F, Michel J, Mattoussi H, Dabbousi B O & Bawendi M G, *Appl Phys Lett,* 70 (1997) 2132.
25 Mekis I, Talapin D V, Kornowski A, Haase M & Weller H, *J Phys Chem B,* 107 (2003) 7454.
26 Cirillo M, Aubert T, Gomes R, Deun R V, Emplit P, Biermann A, Lange H, Thomsen C, Brainis E & Hens Z, *Chem Mater*, 26 (2014) 1154.
27 Zhu H, Michael Z H, Shao L, Yu K, Dabestani R, Zaman M D B & Shijun L, *J Nanomater,* (2014) 14.

28 Yoshino K, Mikami H, Yoneta M & Ikari T, *J Lumin,* 87 (2000) 608.

29 Nam H Y & Han P S, *Phys Rev B,* 59 (1999) 7285.

30 Giner C T, Debernardi A & Cardona M, *Phys Rev B,* 57 (1998) 4664.

31 Meulenberg R W, Jennings T & Stroue G F, *Phys Rev B*, 70 (2004) 235311

32 Dzhagan V M, Valakh M Ya, Raevskaya A E, L Stroyuk A L, Kuchmiy S Ya, D R T Zahn, *Appl Surf Sci*, 255 (2008) 725.

33 Tanaka, A, Onari S & Arai T, *Phys Rev B*, 45 (1992) 6587.